Supplementary data of

Causal interactions between ENSO and the North Tropical Atlantic

Thanh Le[1⋆] and Deg-Hyo Bae[1⋆]

[1]Department of Civil and Environmental Engineering, Sejong University, Seoul 05006, Republic of Korea

⋆Corresponding author(s): Thanh Le (thanhle@sejong.ac.kr) and Deg-Hyo Bae (dhbae@sejong.ac.kr)

Contents of this Supplementary data

Text S1

The North Tropical Atlantic index (NTA) was given as the average sea surface temperature (SST) anomalies in the boreal spring (March-April-May, MAM) over the North Tropical Atlantic region (90°W–20°E; 0°N–15°N). The ENSO index was computed as the average SST anomalies in the Niño 3.4 area (120–170°W; 5°N–5°S) in boreal winter (December–January–February, DJF). Confounding factors (i.e., the Indian Ocean Dipole (IOD) and the Indian Ocean Basin mode (IOB)) may have effects on the connections between NTA and ENSO. The IOD index (Saji *et al* 1999) was given as the difference in boreal fall (September–October–November, SON) sea surface temperature (SST) anomalies between two Indian Ocean regions of the western pole (50–70°E; 10°N–10°S) and southeastern pole (90–110°E; 0°N–10°S). The IOB index is computed as the first empirical orthogonal function (EOF) of boreal spring (MAM) SST anomalies in the Indian Ocean basin (40ºE-120ºE, 20ºN-20ºS).

We use the following multivariate predictive model (e.g., Stern and Kaufmann 2013, Mosedale *et al* 2006) to estimate the causal links between the NTA and ENSO:

$$\boldsymbol{X_t} = \sum_{i=1}^{p} \boldsymbol{\alpha_i X_{t-i}} + \sum_{i=1}^{p} \boldsymbol{\beta_i Y_{t-i}} + \sum_{j=1}^{m} \sum_{i=1}^{p} \boldsymbol{\delta_{j,i} Z_{j,t-i}} + \boldsymbol{\varepsilon_t} \quad \textbf{(1)}$$

where X_t is the NTA (or ENSO index) for year t, Y_t is the ENSO index (or NTA), and $Z_{j,t}$ is the confounding factor j for year t. For example, the NTA for year *1* [i.e., MAM(*1*)] may have predictive power on ENSO for year *1* [i.e., D(*1*)JF(*2*)] and ENSO for year *2* [i.e., D(*2*)JF(*3*)]. Conversely, ENSO for year *0* [i.e., D(*0*)JF(*1*)] may have predictive power on the NTA for year *1* [i.e., MAM(*1*)] and the NTA for year *2* [i.e., MAM(*2*)]. In the predictive model shown in equation 1, while estimating the influence of Y on X (i.e., the contribution of the term $\sum_{i=1}^{p} \beta_i Y_{t-i}$ in predicting X), the contribution of past X events are already taken into account by adding the term $\sum_{i=1}^{p} \alpha_i X_{t-i}$. Thus, the causal influence of Y on X, if detected, is robust and the contribution of past X events are already considered in our analyses.

Here, m is number of confounding factors and $p \geq 1$ is the order of the multivariate predictive model. The optimal order p is computed by minimizing the Schwarz criterion or the Bayesian information criterion (Schwarz 1978). The optimal orders might be different for each model. Here we consider the simultaneous impacts of confounding factors and thus provide more information of the real-world teleconnections. Our analysis uses two different confounding

factors; thus, m is equal to 2. The noise residuals ε_t and the regression coefficients α_i, β_i and $\delta_{j,i}$ are the results of the multiple linear regression analysis using the least squares method. We detrend and normalize all the climate indices.

We estimate the probability of no Granger causality by applying a test of Granger causality (Mosedale *et al* 2006, Stern and Kaufmann 2013, Le and Bae 2019) for the multivariate predictive model shown in equation 1.

For computing the degree of uncertainty, we followed recent guidance (Stocker *et al* 2013, Masson-Delmotte, V., P. Zhai, A. Pirani, S.L. Connors, C. Péan, S. Berger, N. Caud, Y. Chen, L. Goldfarb, M.I. Gomis, M. Huang, K. Leitzell, E. Lonnoy, J.B.R. Matthews, T.K. Maycock, T. Waterfield, O. Yelekçi, R. Yu, and B. ZhouMasson-Delmotte, V., P. Zha 2021) and utilized the terms 'very unlikely', 'unlikely', 'likely' for the 0–10%, 0–33%, and 66–100% probability of the likelihood of the outcome, respectively. For example, if the *p*-value is less than 0.33, the result indicates that ENSO is unlikely to display no Granger causality on NTA. In this instance, we conclude that ENSO has 'causal effect' on NTA.

References

Le T and Bae D H 2019 Causal Links on Interannual Timescale Between ENSO and the IOD in CMIP5 Future Simulations *Geophys. Res. Lett.* **46** 2820–8

Masson-Delmotte, V., P. Zhai, A. Pirani, S.L. Connors, C. Péan, S. Berger, N. Caud, Y. Chen, L. Goldfarb, M.I. Gomis, M. Huang, K. Leitzell, E. Lonnoy, J.B.R. Matthews, T.K. Maycock, T. Waterfield, O. Yelekçi, R. Yu, and B. ZhouMasson-Delmotte, V., P. Zha and B Z 2021 IPCC, 2021: Summary for Policymakers *Climate Change 2021: The Physical Science Basis. Contribution of Working Group I to the Sixth Assessment Report of the Intergovernmental Panel on Climate Change*

Mosedale T J, Stephenson D B, Collins M and Mills T C 2006 Granger Causality of Coupled Climate Processes: Ocean Feedback on the North Atlantic Oscillation *J. Clim.* **19** 1182–94 Online: http://journals.ametsoc.org/doi/abs/10.1175/JCLI3653.1

Saji N H, Goswami B N, Vinayachandran P N and Yamagata T 1999 A dipole mode in the tropical Indian Ocean *Nature* **401** 360–3 Online: http://www.nature.com/articles/43854

Schwarz G 1978 Estimating the dimension of a model *Ann. Stat.* Online: http://projecteuclid.org/euclid.aos/1176344136

Stern D I and Kaufmann R K 2013 Anthropogenic and natural causes of climate change *Clim. Change* **122** 257–69 Online: http://link.springer.com/10.1007/s10584-013-1007-x

Stocker T F, Qin D, Plattner G-K, Alexander L V, Allen S K, Bindoff N L, Bréon F-M, Church J A, Cubasch U, Emori S, Forster P, Friedlingstein P, Gillett N, Gregory J M, Hartmann D L,

Jansen E, Kirtman B, Knutti R, Kumar K K, Lemke P, Marotzke J, Masson-Delmotte, V. Meehl G A, Mokhov I I, Piao S, Ramaswamy V, Randall D, Rhein M, Rojas M, Sabine C, Shindell D, Talley L D, Vaughan D G and Xie S-P 2013 Technical Summary *Climate Change 2013 - The Physical Science Basis* ed Intergovernmental Panel on Climate Change (Cambridge: Cambridge University Press) pp 31–116 Online: https://www.cambridge.org/core/product/identifier/CBO9781107415324A011/type/book_part

Table S1. List of CMIP6 HighResMIP models used in this study

No.	Model name	Modelling center, country	Atmosphere resolution	Ocean resolution
1	BCC-CSM2-HR	BCC, China	0.5° × 0.5° (~ 50 km × 50 km)	0.5° × 0.5°
2	CAMS-CSM1-0	CAMS, China	1° × 1°	1° × 1°
3	CMCC-CM2-HR4	CMCC, Italy	1° × 1°	0.25° × 0.25°
4	CMCC-CM2-VHR4	CMCC, Italy	0.25° × 0.25°	0.25° × 0.25°
5	CNRM-CM6-1	CNRM-CERFACS, France	2.5° × 2.5°	1° × 1°
6	CNRM-CM6-1-HR	CNRM-CERFACS, France	1° × 1°	0.25° × 0.25°
7	ECMWF-IFS-HR	ECMWF, Europe	0.25° × 0.25°	0.25° × 0.25°
8	ECMWF-IFS-LR	ECMWF, Europe	0.5° × 0.5°	1° × 1°
9	FGOALS-f3-H	CAS, China	0.25° × 0.25°	0.1° × 0.1°
10	FGOALS-f3-L	CAS, China	1° × 1°	1° × 1°
11	GFDL-CM4C192	NOAA-GFDL, United States	0.5° × 0.5°	0.25° × 0.25°
12	HadGEM3-GC31-HM	MOHC NERC, United Kingdom	0.5° × 0.5°	0.25° × 0.25°
13	HadGEM3-GC31-LM	MOHC NERC, United Kingdom	2.5° × 2.5°	0.25° × 0.25°
14	HadGEM3-GC31-MM	MOHC NERC, United Kingdom	1° × 1°	0.25° × 0.25°
15	INM-CM5-H	INM, Russia	0.5° × 0.5°	0.1° × 0.1°
16	IPSL-CM6A-ATM-HR	IPSL, France	0.5° × 0.5°	none
17	IPSL-CM6A-LR	IPSL, France	2.5° × 2.5°	1° × 1°
18	MPI-ESM1-2-HR	MPI-M DWD DKRZ, Germany	1° × 1°	0.5° × 0.5°
19	MPI-ESM1-2-XR	MPI-M, Germany	0.5° × 0.5°	0.5° × 0.5°
20	MRI-AGCM3-2-H	MRI, Japan	0.5° × 0.5°	none

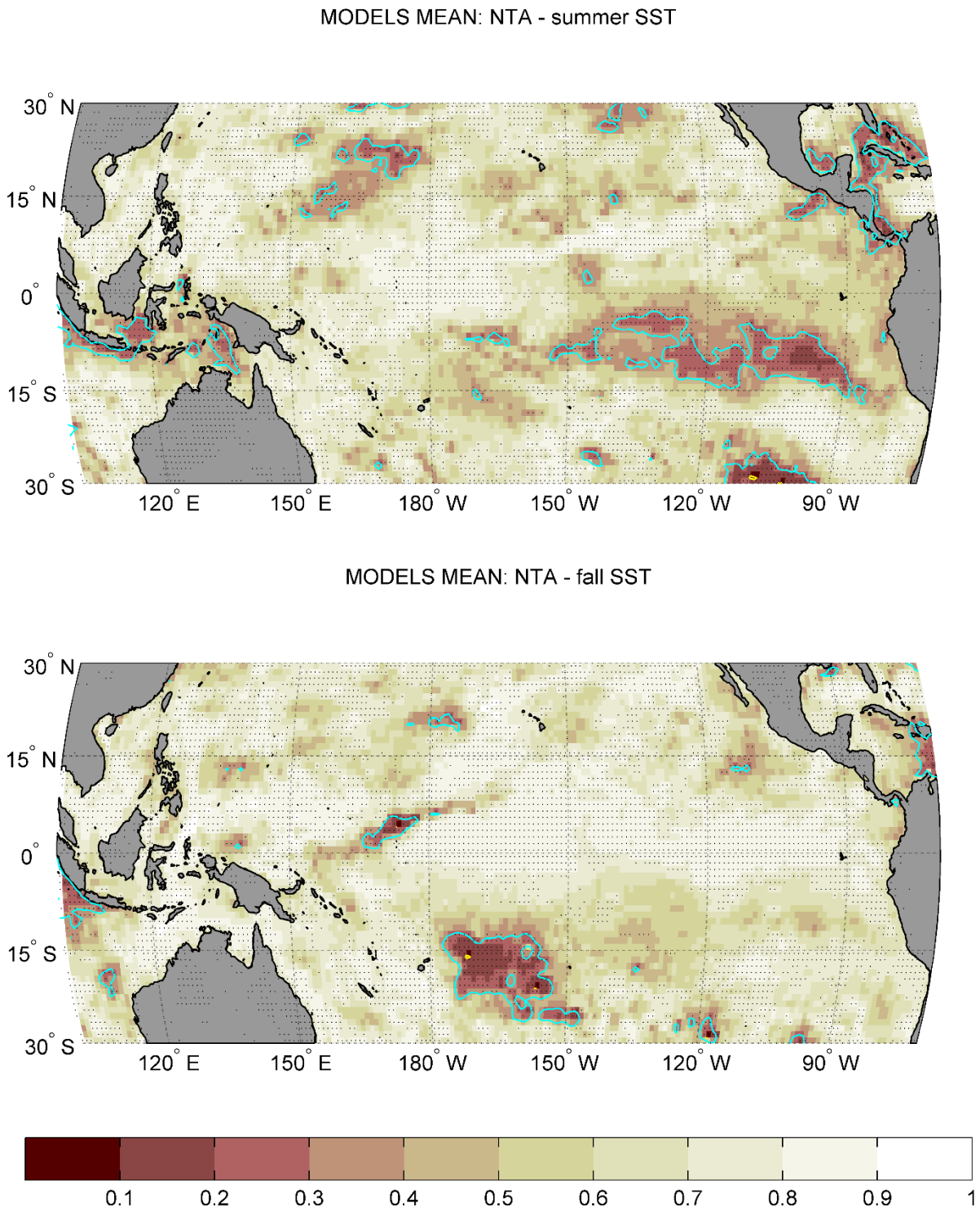

Figure S1. NTA [MAM(t)] effects on boreal summer [JJA(t)] (a) and fall [SON(t)] (b) tropical Pacific SST. The yellow and cyan contour lines specify p value = 0.1 and 0.33, respectively. Brown shades imply low probability for the absence of Granger causality. Stippling designates that more than 70% of models agree on the multi-model mean probability. For a given model, the agreement is defined when the

discrepancy between that model's probability and the multi-model mean probability is less than one standard deviation of the multi-model mean probability. NTA: North Tropical Atlantic; SST: sea surface temperature; MAM: March-April-May; JJA: June-July-August; SON: September-October-November.